Acta Oceanol. Sin., 2022, Vol. 41, No. 2, P. 103–115
https://doi.org/10.1007/s13131-021-1940-x
http://www.aosocean.com
E-mail: ocean2@hyxb.org.cn

A multi-scale high-order recursive filter approach for the sea ice concentration analysis

Lu Yang[1], Dong Li[2]*, Xuefeng Zhang[1], Hongli Fu[2], Kexiu Liu[2]

[1] School of Marine Science and Technology, Tianjin University, Tianjin 300072, China

[2] Key Laboratory of Marine Environmental Information Technology, National Marine Data and Information Service, Ministry of Natural Resources, Tianjin 300171, China

Received 27 February 2021; accepted 12 July 2021

Abstract

With the development and deployment of observation systems in the ocean, more precise passive and active microwave data are becoming available for the weather forecasting and the climate monitoring. Due to the complicated variability of the sea ice concentration (SIC) in the marginal ice zone and the scarcity of high-precision sea ice data, how to use less data to accurately reconstruct the sea ice field has become an urgent problem to be solved. A reconstruction method for gridding observations using the variational optimization technique, called the multi-scale high-order recursive filter (MHRF), which is a combination of Van Vliet fourth-order recursive filter and the three-dimensional variational (3D-VAR) analysis, has been designed in this study to reproduce the refined structure of sea ice field. Compared with the existing spatial multi-scale first-order recursive filter (SMRF) in which left and right filter iterative processes are executed many times, the MHRF scheme only executes the same filter process once to reduce the analysis errors caused by multiple filters and improve the filter precision. Furthermore, the series connected transfer function in the high-order recursive filter is equivalently replaced by the paralleled one, which can carry out the independent filter process in every direction in order to improve the filter efficiency. Experimental results demonstrate that this method possesses a good potential in extracting the observation information to successfully reconstruct the SIC field in computational efficiency.

Key words: Van Vliet fourth-order recursive filter, multi-scale recursive filter, sea ice concentration

Citation: Yang Lu, Li Dong, Zhang Xuefeng, Fu Hongli, Liu Kexiu. 2022. A multi-scale high-order recursive filter approach for the sea ice concentration analysis. Acta Oceanologica Sinica, 41(2): 103–115, doi: 10.1007/s13131-021-1940-x

1 Introduction

Background error covariance matrix plays an important role in oceanographic 3D-VAR data assimilation, which determines the correction degree of the analyzed field relative to the background field. In order to reduce the memory and computation overhead, the recursive filter is usually used to simulate the background error covariance matrix (Lorenc, 1992; Hayden and Purser, 1995; Huang, 2000; Purser et al., 2003a, b), which avoids resolving the explicit inversion of the background error covariance matrix based on statistical method with the storage of large matrix.

Theoretically, the recursive filter in the 3D-VAR should be anisotropic (Li et al., 2011), which allows more freedom degrees in adaptively defining the error statistics (Purser et al., 2003a; Gao et al., 2004). However, it is usually difficult to determine the coefficients of anisotropic filters via statistical methods in practical applications, seeing that the process of constructing such filters satisfying the requirements of the variational analysis is too complicated. Therefore, the background error covariance is commonly expressed as spatially homogeneous and isotropic Gaussian function in realistic applications (Derber and Rosati, 1989; Masina et al., 2001; Huang et al., 2002). Hayden and Purser (1995) extended the work of Purser and McQuigg (1982) and Lorenc (1992), showing how a series of simple and relative computation-cheap recursive filters could produce empirical isotropic smoothers. In the ocean data assimilation field, the recursive filter commonly used in the 3D-VAR is actually the first-order repeated multiple filtering (that is, the series of multiple first order filters) to simulate the Gaussian filter (Zhang et al., 2020). It is simple in form and easy to use, so it has been widely used in the field of ocean data assimilation. However, the filter accuracy constructed by the first-order filter is relatively low. Theoretically, the cascading recursive filter should be extended to the infinity in the filtering process, yet the actual input data is of finite length sequence. Once it is truncated, there will remain a large error in the calculation result. There are usually two ways to cope with this problem: one is to extend the finite input sequence to an extra length related to the correlation length L, inducing a lot of extra computational burden with the increasing of L; the other refers to the study of Hayden and Purser (1995). After each left filter is completed, an estimate for the left boundary of the input sequence at this time is given before the next right filter is executed. However, it is difficult to estimate the boundary with the increase of filtering times.

In recent years, the high-order recursive filter is mostly used to replace the first-order filter for multiple filtering in the field of ocean data assimilation. Among them, the commonly used high-order filter is Purser recursive filter, which carries out Taylor expansion on the transfer function of Gaussian filter to construct the high-order isotropic Gaussian recursive filter. However, the

Foundation item: The National Key Research and Development Program of China under contract Nos 2018YFC1407402 and 2017YFC1404103; the National Programme on Global Change and Air-Sea Interaction (GASI-IPOVAI-04) of China; the Open Fund Project of Key Laboratory of Marine Environmental Information Technology, Ministry of Natural Resources.
*Corresponding author, E-mail: lidong2003@gmail.com

calculation is too complicated to control the filter parameters in the practical applications.

In order to solve the above problems, a reconstruction method based on variational optimization technology, the multi-scale high-order recursive filter scheme (MHRF), is designed, which refers to the research results of filtering theories, such as the Van Vliet fourth-order recursive Gaussian filter proposed by Van Vliet et al. (1998) and the spatial multi-scale first-order recursive filter (SMRF) scheme proposed by Zhang et al. (2020). The MHRF scheme adopts the Van Vliet fourth-order recursive Gaussian filter to replace the first-order recursive filter in the SMRF scheme via transforming the series high-order recursive filter into the parallel of the low-order recursive filter. Due to the use of high-order filter, it is not necessary to carry out multiple right and left filter as the first-order filter. At the same time, because the high-order filter is converted into a parallel form, the right filter and the left filter are independent, meaning that there is no series relation so that the independent filtering processing is realized in every direction. Therefore, the high-order recursive filter can avoid the boundary problem mentioned above and achieve better the approximation effect of Gaussian filter. In addition, the MHRF scheme also retains advantages in the SMRF scheme: first, the convergence property is implied in the minimization process; second, the weight parameters are automatically determined by the line search algorithm without manual intervention; the last, the information of different observation scales can be extracted continuously in an iterative process.

The paper is organized as follows. In Section 2, the principle of Van Vliet fourth-order recursive Gaussian filter is introduced firstly. Then, the principle of the SMRF scheme is briefly reviewed. Finally, the Van Vliet recursive filter is applied to the multi-scale 3D-VAR analysis, and the MHRF scheme is proposed. In Section 3, the MHRF scheme is preliminarily tested by single point observation. In Section 4, MHRF scheme is further applied to the construction of Arctic sea ice concentration field, and the MHRF scheme and SMRF scheme are compared in detail in terms of analyzed field error and calculation efficiency. The conclusions are summarized in Section 5.

2 Method

2.1 *Van Vliet fourth-order recursive Gaussian filter*

Van Vliet recursive Gaussian filter has been widely applied in the field of computer graphics and image processing because of its simple calculation, convenience and efficiency.

The impulse response is a Gaussian filter of the following form:

$$h(t;\sigma)=\frac{1}{\sqrt{2\pi}\sigma}\mathrm{e}^{\frac{-t^2}{2\sigma^2}}, \tag{1}$$

where $h(t;\sigma)$ is the Gaussian function of the pulse signal associated with t and σ. Where t is time, $\sigma^2=\alpha^2/4\pi$, α is the shaping factor of the Gaussian pulse.

The transfer function of Van Vliet fourth-order digital filter is expressed as

$$\begin{cases} H(z)=H_+(z)\cdot H_-(z), \\ H_+(z)=\dfrac{\alpha}{1+\sum\limits_{i=1}^{4}b_i z^{-i}}, \\ H_-(z)=\dfrac{\alpha}{1+\sum\limits_{i=1}^{4}b_i z^{i}}, \end{cases} \tag{2}$$

$$\begin{cases} b=\prod\limits_{i=1}^{4}d_i^{-1}, \\ b_1=-b\sum\limits_{i=3}^{4}\sum\limits_{j=2}^{i-1}\sum\limits_{k=1}^{j-1}d_i d_j d_k, \\ b_2=b\sum\limits_{i=2}^{4}\sum\limits_{j=1}^{i-1}d_i d_j, \\ b_3=-b\sum\limits_{i=1}^{4}d_i, \\ b_4=b, \\ \alpha=1+\sum\limits_{i=1}^{4}b_i, \end{cases} \tag{3}$$

where d_1、d_2、d_3、d_4 are the poles of $H_-(z)$. When $\sigma=\sigma_0=2$, d_1、d_2、d_3、d_4 are:

$$\begin{aligned} d_1(\sigma_0)&=1.132\ 28+1.281\ 14i, \\ d_2(\sigma_0)&=d_1^*, \\ d_3(\sigma_0)&=1.785\ 34-0.467\ 63i, \\ d_4(\sigma_0)&=d_3^*, \end{aligned}$$

where $(\cdot)^*$ indicates conjugate.

The above is for the case of $\sigma=\sigma_0=2$. When σ is an arbitrary value, set the parameter $q=\dfrac{\sigma}{\sigma_0}$. Then, according to the scale transformation property of Fourier transform, d_1、d_2、d_3、d_4 are indicated as

$$\begin{cases} d_1(\sigma)=d_1(\sigma_0)^{\frac{1}{q}}, \\ d_2(\sigma)=d_1^*(\sigma), \\ d_3(\sigma)=d_3(\sigma_0)^{\frac{1}{q}}, \\ d_4(\sigma)=d_3^*(\sigma). \end{cases} \tag{4}$$

After d_1、d_2、d_3、d_4 are calculated, the coefficients of the filter can be calculated by Eq. (3).

According to Eq. (2), the right and left filter processes go through in Van Vliet fourth-order recursive Gaussian filter, which is equivalent to the cascade of two fourth-order recursive filters. The transfer function $H(z)$ of the filter is decomposed into parallel form. The poles of $H_+(z)$ are the reciprocal of the poles of $H_-(z)$. Since the poles of $H(z)$ are conjugated in pairs, it has the following decomposition form:

$$H(z)=H_1(z)+H_2(z)+H_3(z)+H_4(z), \tag{5}$$

$$\begin{cases} H_1(z)=\dfrac{e_1 z+f_1}{(z-d_1)(z-d_2)}, \\ H_2(z)=\dfrac{e_2 z+f_2}{(z-d_3)(z-d_4)}, \\ H_3(z)=\dfrac{e_3 z+f_3}{(1-d_1 z)(1-d_2 z)}, \\ H_4(z)=\dfrac{e_4 z+f_4}{(1-d_3 z)(1-d_4 z)}, \end{cases} \tag{6}$$

where e_i、$f_i(i=1,2,3,4)$ are the undetermined coefficient, which can be obtained through calculation:

$$\begin{cases} e_1 = 2\,\mathrm{Re}\,(c_1)\,, \\ e_2 = 2\,\mathrm{Re}\,(c_2)\,, \\ e_3 = -2\,\mathrm{Re}\,(c_3 d_2)\,, \\ e_4 = -2\,\mathrm{Re}\,(c_4 d_4)\,, \\ f_1 = -2\,\mathrm{Re}\,(c_1 d_2)\,, \\ f_2 = -2\,\mathrm{Re}\,(c_2 d_4)\,, \\ f_3 = 2\,\mathrm{Re}\,(c_3)\,, \\ f_4 = 2\,\mathrm{Re}\,(c_4)\,, \\ c_1 = H_+ d_1 \cdot \dfrac{\alpha d_1^4}{(d_1 - d_2)(d_1 - d_3)(d_t - d_4)}, \\ c_2 = H_+ d_1 \cdot \dfrac{\alpha d_3^4}{(d_3 - d_1)(d_3 - d_2)(d_3 - d_4)}, \\ c_3 = c_1 d_1^{-1}, \\ c_4 = c_2 d_3^{-1}, \end{cases} \tag{7}$$

where $\mathrm{Re}(\cdot)$ indicates the real part of the complex number.

Based on Eqs (5) and (6), the one-dimensional fourth-order Gaussian filter is decomposed into four parallel second-order recursive filters. Among them, $H_1(z)$ and $H_2(z)$ are left filters, $H_3(z)$ and $H_4(z)$ are right filters, and the four filter processes can be performed independently in parallel. Because d_1, d_2, d_3 and d_4 are located in the unit circle in the complex plane, these four filtering processes are stable.

2.2 *Multi-scale high-order recursive filter 3D-VAR*

The traditional 3D-VAR method is difficult to extract multi-scale observation information. The multigrid 3D-VAR method (Li et al., 2008) and sequential recursive filter 3D-VAR method (He et al., 2008) can extract the multi-scale information from long wave to short wave successively via carrying out a series of 3D-VAR analyses. The multi-scale first-order recursive filter 3D-VAR (SMRF) is another method that can achieve multi-scale information extraction via carrying out 3D-VAR analysis once (Zhang et al., 2020).

The variational optimization technique is used to minimize the difference between the estimated field and the observed field in the SMRF scheme. The unconstrained minimization problem is as follows:

$$\min J(x) = \min \frac{1}{2} (x^\circ - \mathbf{H}x)^{\mathrm{T}} R^{-1} (x^\circ - \mathbf{H}x)\,, \tag{8}$$

where x is the analyzed field, x° is the observed field, $\mathbf{H}$ is an interpolation operator from analysis space to observation space, R is the observational error covariance matrix, $(\cdot)^{\mathrm{T}}$ indicates transpose, and $(\cdot)^{-1}$ indicates inversion, the gradient of $J(x)$ is

$$\nabla J(x) = -\mathbf{H}^{\mathrm{T}} R^{-1} (x^\circ - \mathbf{H}x)\,. \tag{9}$$

Once the gradient is obtained according to Eq. (9), the unconstrained minimization problem Eq. (8) then can be solved by using a minimization algorithm such as the steepest descent method, the Limited-memory BFGS (L-BFGS) method or the conjugate gradient method.

In order to further suppress the observation noise, let $x = \mathbf{B}w$ in Eq. (8), where $\mathbf{B}$ represents the recursive filtering operator. Then the problem described in Eq. (8) is replaced by

$$\min J(w) = \min \frac{1}{2} (x^\circ - \mathbf{HB}w)^{\mathrm{T}} R^{-1} (x^\circ - \mathbf{HB}w)\,. \tag{10}$$

In this case, the gradient of the cost function is expressed as

$$\nabla J(w) = -\mathbf{BH}^{\mathrm{T}} R^{-1} (x^\circ - \mathbf{HB}w)\,. \tag{11}$$

As Zhang et al. (2020) pointed out, due to the "flawed" gradient arising from the irregular data distribution, the analyzed field obtained by solving Eq. (10) using the minimization algorithm will lose the coherent long wave characteristics in the data-void region. Therefore, in addition to applying the first-order recursive filter to the variable w, the SMRF scheme applies another first-order recursive filter to the gradient of the cost functional $\nabla J(w)$ at each iteration of a minimization procedure. With the increase of the number of iterations, the filter parameter α gradually decreases from a big value to a small value. Then, observation information, from longer to shorter wavelengths, can be extracted successively. The algorithm is simply described as follows:

(1) Give an initial guess value $w = w_0$, then choose a small filter parameter β and a large enough one denoted as α.

(2) Calculate $\mathbf{B}w$ by applying a recursive filter operator $\mathbf{B}$ with the parameter β to w.

(3) Calculate the cost function $J(w)$ and its gradient $\nabla J(w)$.

(4) Apply another recursive filter operator $\mathbf{E}$ with the parameter α to $-\nabla J(w)$, yielding $\mathbf{E}(-\nabla J(w))$.

(5) Select $\mathbf{E}(-\nabla J(w))$ as the descent direction during minimization, and use a line search algorithm (Moré and Thuente, 1994) to find the appropriate step size l, then w is adjusted to $w = w + l \cdot \mathbf{E}(-\nabla J(w))$.

(6) Decrease the value of α.

(7) Loop from step (2) until the convergence criterion is met.

(8) The final analysis is $x = \mathbf{B}w$.

2.3 *The MHRF scheme*

Based on the theory of Van Vliet fourth-order recursive Gaussian filter, the SMRF scheme is improved in this study. The cascade of multiple first-order filters in the SMRF scheme is replaced by the parallel of four second-order filters constructed by Eqs (5) and (6) to simulate the Gaussian filter, and the MHRF scheme is designed. The algorithm is modified as a flow chart shown in Fig. 1.

We now give a brief analysis on the fundamentals of this scheme. Similar to the SMRF scheme, at the beginning, w is given an initial guess value w_0 and a small parameter β and a large parameter α are given (β and α have the same meanings and both represent the exponential part of d in Eq. (4). But β is a fixed value and α decreases with the increase of iteration times). Then, the gradient $\nabla J(w_0)$ is calculated by applying Van Vliet high-order recursive filter with parameter β to w. In fact, this is a very weak filtering process because the parameter β is a very small value. Therefore, most of the observation information are kept in $\nabla J(w_0)$. In other words, $\nabla J(w)$ in Eq. (11) actually represents the observation residual at w (observation residual refers to the remaining observation information after deducting the currently extracted information in the observation). Then, another recursive filter operator $\mathbf{E}$ with the large parameter α is applied to the negative direction of the gradient $-\nabla J(w_0)$ to obtain $\mathbf{E}(-\nabla J(w_0))$. Actually, $\mathbf{E}(-\nabla J(w_0))$ represents the "longest" wavelength information of the observed residuals at $w = w_0$ because the initial coefficient α is large enough. In addition, since the filtering operator is positive definite, $\mathbf{E}(-\nabla J(w_0))$ is guaranteed to be a descent direction which insures the decrease of the residual difference between the estimated value and the observed value along this direction. A line search procedure is performed along this direction to find an appropriate step length l. When the estimate is updated by $w_1 = w_0 + l \times (-\nabla J(w_0))$, the observed residual at $w = w_0$ is "fully" extracted and incorporated into the new estimate w_1. In the next iteration, the parameter α is reduced, so the

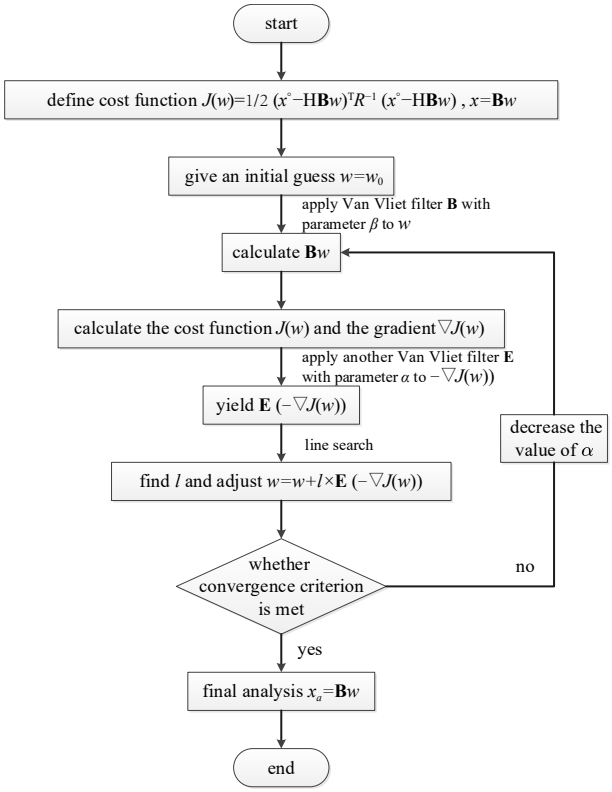

Fig. 1. A flow chart of the MHRF scheme.

"longest" wavelength of the observed residuals at $w = w_1$ is extracted and superposed with w_1 to generate w_2. As the iteration proceeds, the information of all wavelengths can be fully "extracted" in turn and incorporated into the final analysis value.

Since the Van Vliet high-order recursive filter is applied in the MHRF scheme, it is not necessary to carry out multiple right and left filters as the first-order filter used in the SMRF scheme. It only needs to perform the filtering process once. Accordingly, this method avoids the problem that the boundary is difficult to estimate in the multiple filters. Because the high-order filter is transformed into a parallel form, the right filter and the left filter are independent and there is no series relation between them, meaning high computational efficiency.

Although the gradient in the MHRF scheme is an isotropic filter, the filter parameter α changes with the number of iterations to extract different scale information. Therefore, the cumulative effect of the whole iteration procedure is actually characterized by non-uniform anisotropic filter. In other words, it can achieve strong filter in sparse observation area and its surrounding area to extract long wavelength information and weak filter in dense observation area to avoid losing short wavelength information.

3 Single-observation ideal experiment

As mentioned in Section 2.3, the biggest difference between the MHRF scheme and the SMRF scheme is that they use different filters, in which one is Van Vliet high-order recursive filter and the other is first-order recursive filter. In order to compare the ability of the two filters to simulate the Gaussian function, a set of one-dimensional recursive filter experiment is designed, as shown in Section 3.1. In addition, in order to further explore the ability in propagating observation signals for the MHRF scheme, two-dimensional single-observation ideal experiment is carried out, as shown in Section 3.2. For comparison, the L-BFGS algorithm based on the Van Vliet high-order recursive filter is also used to solve Eq. (10) in Section 3.2.

3.1 *One-dimensional recursive filter experiment*

In this section, the range of the experiment domain is [0, 10]. One point is taken every 0.25 length and there is a total of 41 grid points. The observed value of the 21st grid point at the center of this domain is given as 1.0.

In Figs 2a, b and c, the dotted lines are respectively the results from the first-order recursive filter once (the filter parameter α is given 0.6), the first-order recursive filter four times (the filter parameter α is given 0.5) and the Van Vliet high-order recursive filter once (the filter parameter α is given 2.6). The solid line in Fig. 2 is the calculation result of Gaussian function when the expected value is 5 and the variance is 1.5. Compared with the result from the first-order recursive filter once, the result from the Van Vliet fourth-order recursive filter is closer to the Gaussian function and has higher accuracy. However, the simulation effect of the first-order recursive filter is significantly improved after increasing of filtering times (Fig. 2b). When the filtering times is increased to four, the result is better than that of the Van Vliet fourth-order recursive filter. But the cost of time cannot be ignored. In general, the Van Vliet fourth-order filter shows good performance in both the approximation effect of Gaussian function and the operation efficiency.

3.2 *Two-dimensional single-observation experiment*

3.2.1 *Data and parameters*

The analysis domain covers a square region with longitude range of 0°–10°E and latitude range of 0°–10°N. The grid resolution is 0.25°×0.25. The grid size is 41 × 41. We place only one observation with its value equal to 1.0 at the center of this domain and the position is 5°N, 5°E. The parameter α in the MHRF scheme is chosen as the following Gaussian function:

$$\alpha = \alpha_{\max} \cdot \mathrm{e}^{-\frac{i^2}{2\tau^2}} + c, \quad i = 0, 1, \cdots, N, \tag{12}$$

where i represents the iteration number, N is a constant and the total number of iterations, $\tau = \dfrac{N}{4}$, $\alpha_{\max} = 15$. In order to prevent the exponential part of d in Eq. (4) from being too large when α approaches 0, the constant c is added after the Gaussian function. Here, c is given as 1.0. As we can see, $\alpha = \alpha_{\max}\ (i = 0)$, then α approaches 1.0 when $i = N$. In this experiment we set N=60. The observation operator H is obtained by bilinear interpolation. The initial-guess field w_0 is set to zero.

3.2.2 *Results*

Figure 3 shows the results of solving Eq. (10) by L-BFGS algorithm when the Van Vliet high-order recursive filtering parameters β=1, 2, 4 and 6, respectively. It can be seen that the accuracy and universality of observation signal propagation depend on different β. If β is small (Fig. 3a), the analysis approaches the observation closely and the details involved in the observation can be maximized. At the same time, an obvious problem is that it has a very small signal propagation range and it can only capture information in short waves. If it is applied in the actual observation, the observation signal cannot propagate in data-void regions. On the contrary, when β is relatively large (Fig. 3d), although the observation signal can propagate to more wide range of areas, the accuracy of the analysis will be lost in the practical application. To sum up, we need not only a small parameter to ensure maximum observation details, but also a large parameter to fill in the data-sparse or data-void regions through long wave

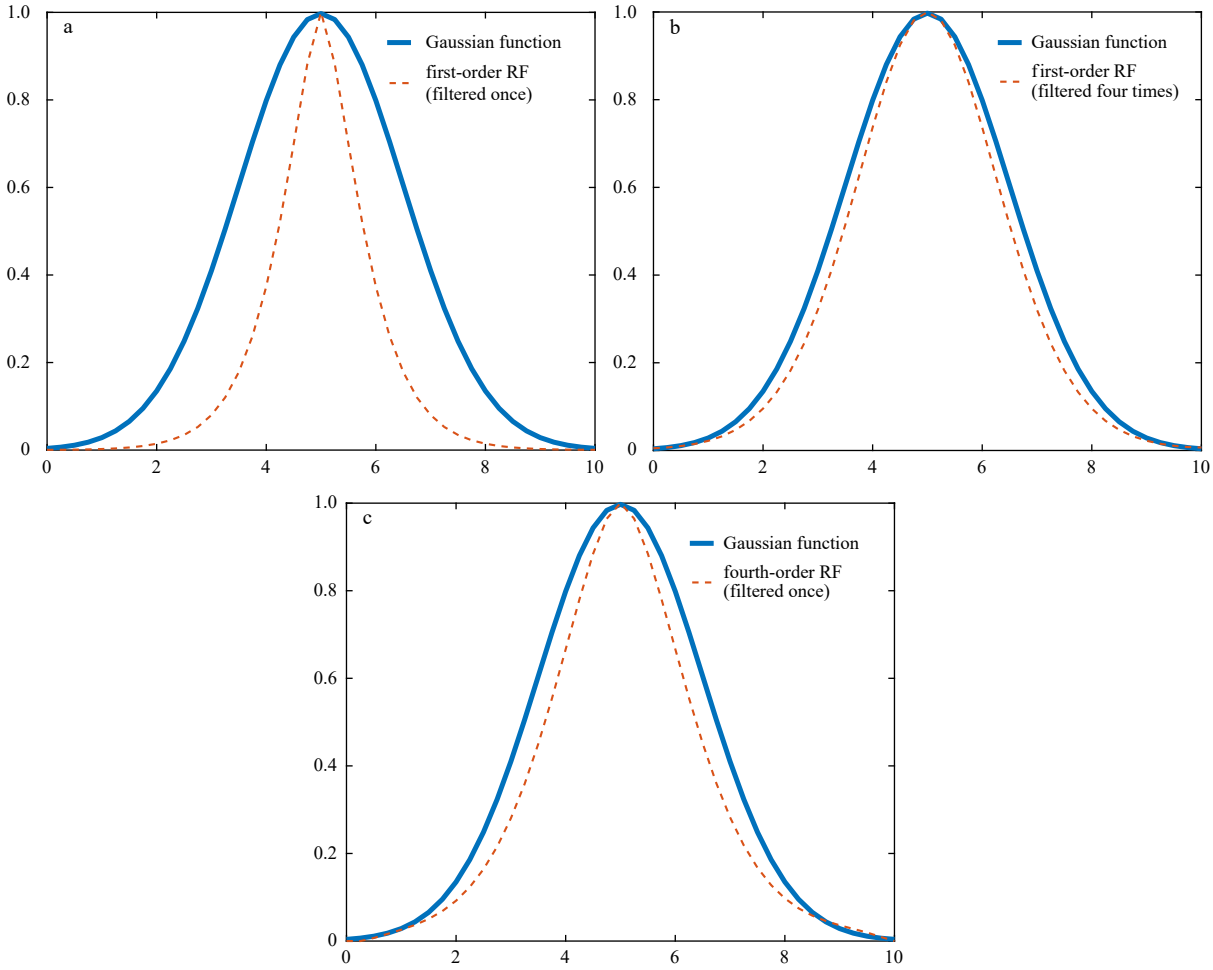

Fig. 2. Comparison of one-dimensional recursive filter results (dotted line) with the Gaussian function (solid line): the first-order recursive filter once (a); the first-order recursive filter four times (b); Van Vliet fourth-order recursive filter once (c).

analysis. The MHRF scheme we designed can meet this requirement to some extent.

Figure 4 shows the observation signal propagation results of the MHRF scheme at different iterations using a small parameter β (0.97). As the iterations gradually increase in Figs 4a–d, the analysis is corrected from the large-scale signals to detail. Compared with the single-scale signal propagation process depending on parameter selection in Fig. 3, the MHRF scheme can analyze data of all scales once. The extraction of small-scale signals ensures the accuracy of analysis results, while the extraction of large-scale signals enables the observation signals to propagate to more wide range of areas.

4 Application to sea ice concentration experiment

4.1 *Data and parameters*

The ice concentration observations used in the analysis are derived from US Defense Meteorological Satellite Program (DMSP) 5D-3/F-18 Special Sensor Microwave Imager/Sounder (SSMIS) passive microwave data, processed by the National Snow and Ice Data Center with the NASA Team algorithm (Cavalieri et al., 2012). The data set is named Near-Real-Time DMSP SSMIS Daily Polar Gridded Sea Ice Concentrations, Version 1(Maslanik and Stroeve, 1999). The time resolution is 1 d and the spatial resolution is 25 km×25 km. The data cover the South Pole and North Pole.

The "true" state of the Arctic SIC field constructed from the SMMIS SIC on August 10, 2020 is shown in Fig. 5a. Since the spatial resolution of the analysis field is usually different from the satellite observation, we choose one observation for every four analysis grid points. In order to examine the validation of the MHRF scheme, we also remove partial points located in the sea ice marginal region. Therefore, there are 1 384 observations (Fig. 5b) remained to restore the "true" field. The parameters of the MHRF scheme are $\theta = 0.99$, $\sigma_{\max} = 18$, $N = 125$. The other parameters are the same as those of two-dimensional single-observation experiment.

4.2 *Results of the L-BFGS scheme*

Figure 6 shows the SIC analyzed field obtained by L-BFGS algorithm based on the Van Vliet fourth-order recursive filter with different parameter β values. It can be seen that when β is large, the observed long-wave information is extracted, but the analysis result is too smooth to reflect the short-wave information compared with the SIC "true" field in Fig. 5a. When β is small, although the detailed information in the observation is extracted, the range of signal propagation from each observation point to the surrounding area is small so that the data hole area lacks effective observation information. In addition, the descent directions at iterations 2, 4 and 8 for Fig. 6a suggest that the irregular distribution of observations can lead to the gradient "jump" and the spatial discontinuous distribution in the data-void region (Figs 7b, d and f). Ac-

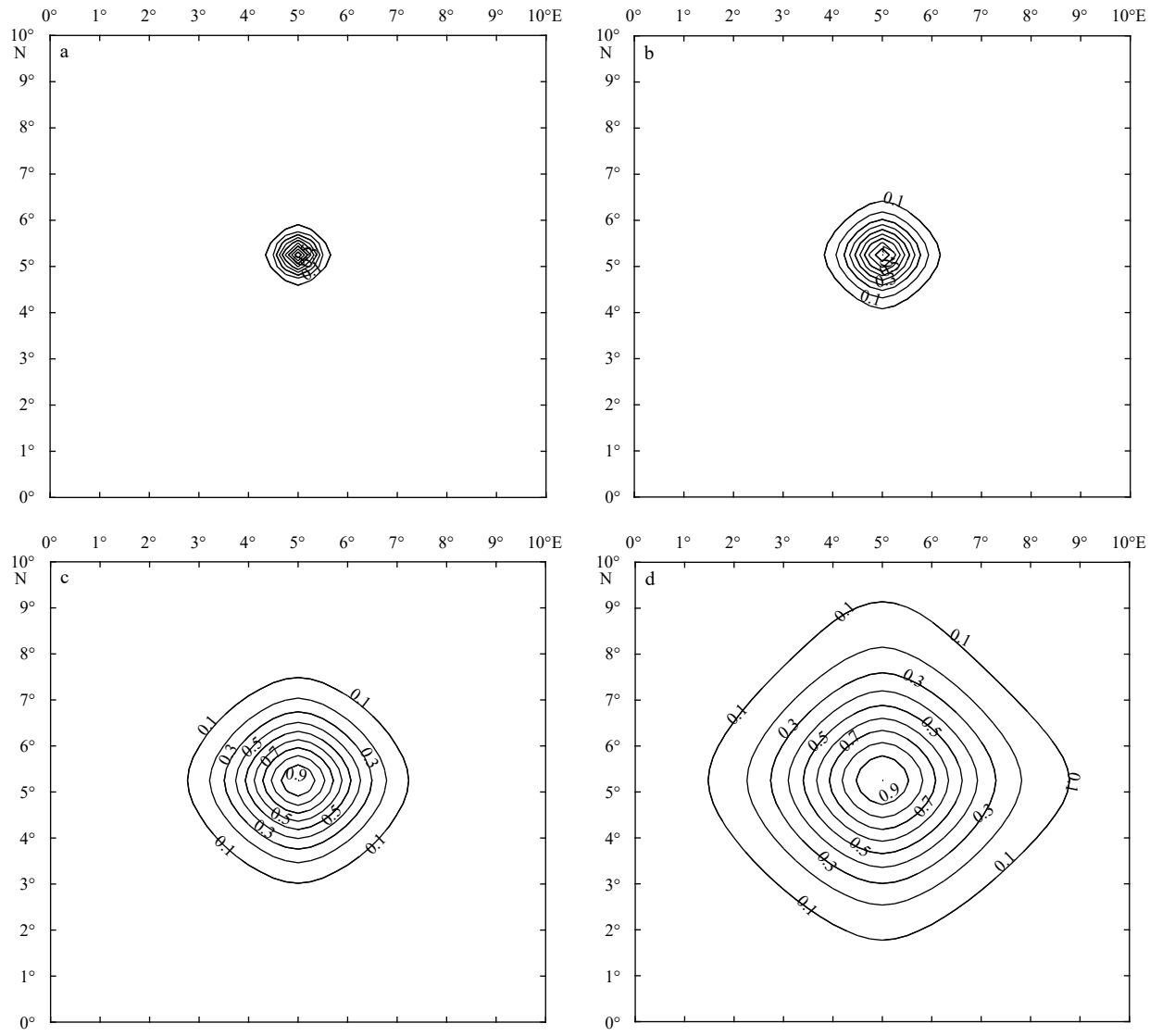

Fig. 3. The spread of observational information using the L-BFGS scheme when β= 1 (a), 2 (b), 4 (c) and 6 (d), respectively.

cordingly, there analyses updated along this direction tend to the incoherent structure and data holes are not properly filled. The same problem will exist for other gradient-based minimization algorithms.

4.3 *Results of the MHRF scheme*

When the parameter β =0.99 and the total number of iterations N =125, the analyzed field from the MHRF scheme (Fig. 8b) is very similar to the "true" field in Fig. 8a. Compared with the sharp variation of the gradient of the L-BFGS scheme in the data-void region (Figs 7b, d, and f), the MHRF scheme extracts the long wavelength from the observed residual to establish the descent direction. With the increase of iterations, the parameter σ gradually decreases. Then the descent direction calculated by Gaussian filtering of the gradient can be obtained successively from longer to shorter wavelengths (Figs 9b, d and f), which effectively fills the defect of the gradient in the data-void region. Accordingly, the analyzed field adjusted along this direction can also be extracted successively (Figs 9a, c, and e). At the end of the iteration, the observation information of each wavelength is merged into the final analyzed field, which not only retains the detailed short wavelength information in the observation, but also fills up the value of in the data-void region well. The SIC field is reconstructed successfully.

4.4 *Comparison between the MHRF scheme and the SMRF scheme*

In this section, two-dimensional SIC experiment is carried out for the SMRF scheme. The analyzed field is shown in Fig. 10b where the filter parameter β is 0.2, the initial maximum value of another filtering parameter α is 0.9 and N=500. According to Figs 8b and 10, as multi-scale recursive filter 3D-VAR methods, the MHRF scheme and the SMRF scheme both show good performance in extracting multi-scale information.

The differences between the analyzed field and the "true" field in the two schemes are shown in Fig. 11. The MHRF scheme tends to underestimate the SIC value, such as the lack of observation area near 85°N, 60°W in Fig. 11a. However, the SMRF scheme prefers to overestimate the SIC value, as shown near 82°N, 65°W in Fig. 11b. This phenomenon is more intuitive in the histogram of the deviation between the analyzed field and the true SIC field in Fig. 12. The number of deviations in the interval [0.3, 0.1) of the MHRF scheme is greater than the SMRF scheme, while in

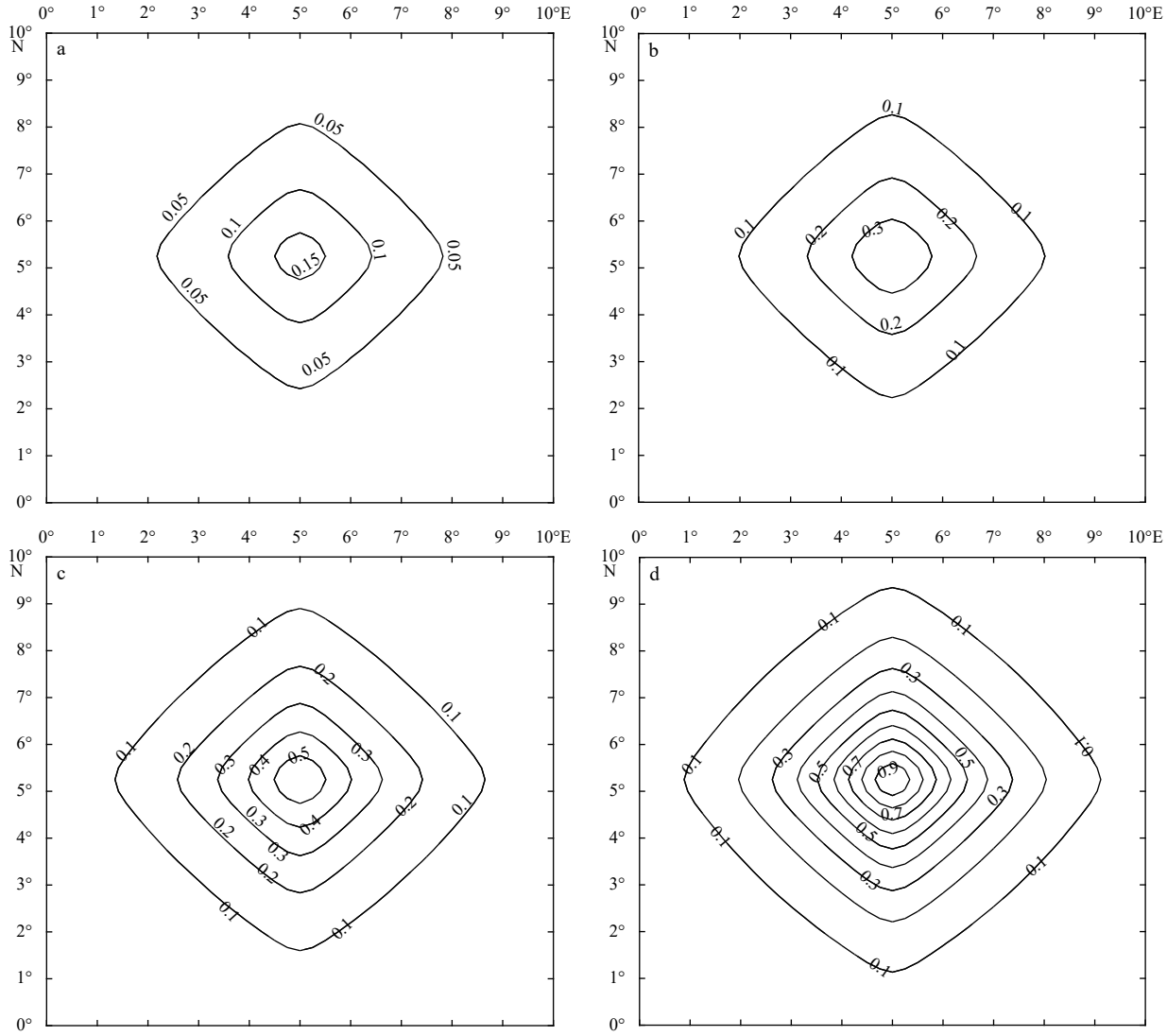

Fig. 4. The spread of observational information in the multi-scale high-order recursive filter scheme when θ= 0.97. a–d are the results at iteration 2, 5, 8 and 24, respectively.

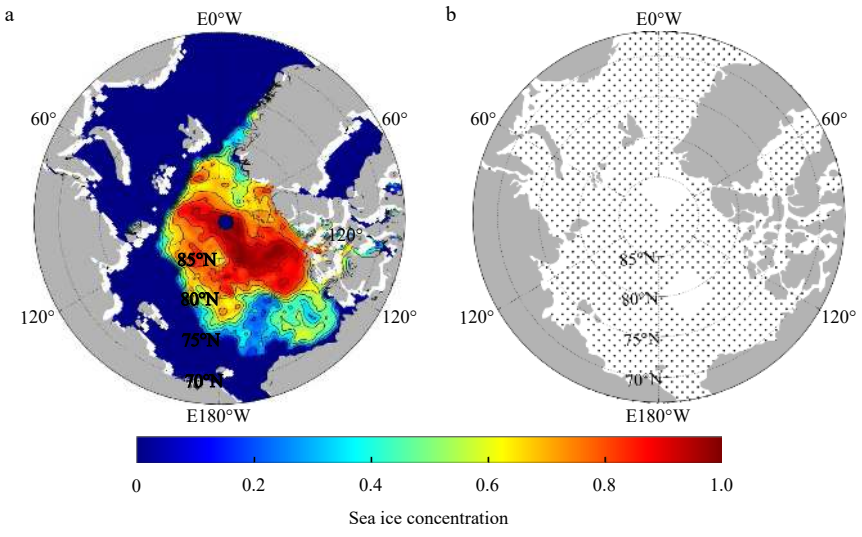

Fig. 5. The true SIC field of the Arctic Ocean constructed based on the SSMIS SIC on August 10, 2020 (a), and the locations of "observations" (b).

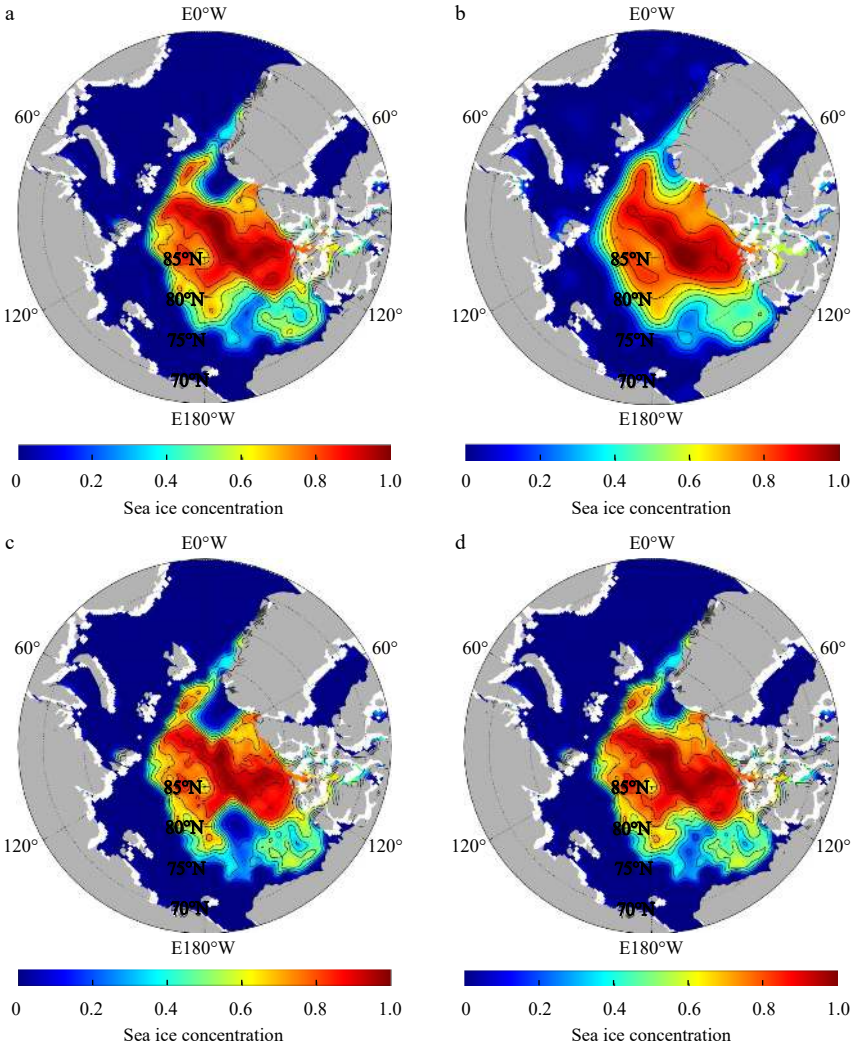

Fig. 6. Analyzed field solved by using the L-BFGS scheme when β=4 (a), 10 (b), 15 (c) and 25 (d).

the interval [0.1, 0.3) is less. In addition, although the root mean square error (RMSE) between the analyzed field and the true SIC field in the MHRF scheme is 0.001 1 larger than that of the SMRF scheme (Table 1), the number of deviations in the MHRF scheme is more than that of the SMRF scheme not only in the interval [–0.1, 0.1) but also in the interval [–0.3, 0.3) (Fig. 12), accounting for 99.2%. In general, the MHRF scheme is superior to the SMRF scheme, except that there is a certain deviation between the analyzed value of a few grid points and the observation "true" value.

The RMSE is calculated as follows:

$$\mathrm{RMSE}=\sqrt{\frac{\sum_{i=1}^{n}(y_i-x_i)^2}{n}}, \tag{13}$$

where i is index of the grid point, y_i is the analyzed value at the i th grid point, x_i is the observation value at the i th grid point, n denotes the total number of grid points (except land points and the north pole center point).

It is particularly noteworthy that the MHRF scheme transforms the high-order filter into a parallel form so that the right filter and the left filter are independent and the filtering process is only performed once in each direction, which makes the analyzed field with only 125 iterations can reach the accuracy of the SMRF scheme with 500 iterations. In the performance of central processing unit (CPU) computation time, the MHRF scheme is only 1/8 of the SMRF scheme.

5 Conclusions and discussion

In this paper, the MHRF scheme is designed based on the theory of the Van Vliet fourth-order recursive Gaussian filter and multi-scale first-order recursive filter method. It uses four second-order filters in parallel to replace the series of multiple first-order filters in the SMRF scheme to simulate the Gaussian filter. In this method, the gradient of the cost function is filtered once and the descent direction is established by extracting the long wave of the observation residuals. With the decrease of the parameters, the observation information can be gradually extracted. Based on the MHRF scheme, the analyzed field of SIC is successfully reconstructed by extracting the observation from longer to shorter wavelength and the CPU calculation time is only 1/8 of the SMRF scheme.

The main conclusions can be summarized as follows:

(1) Based on the Van Vliet recursive Gaussian filter theory, the high-order filter in the series form is converted into the parallel of

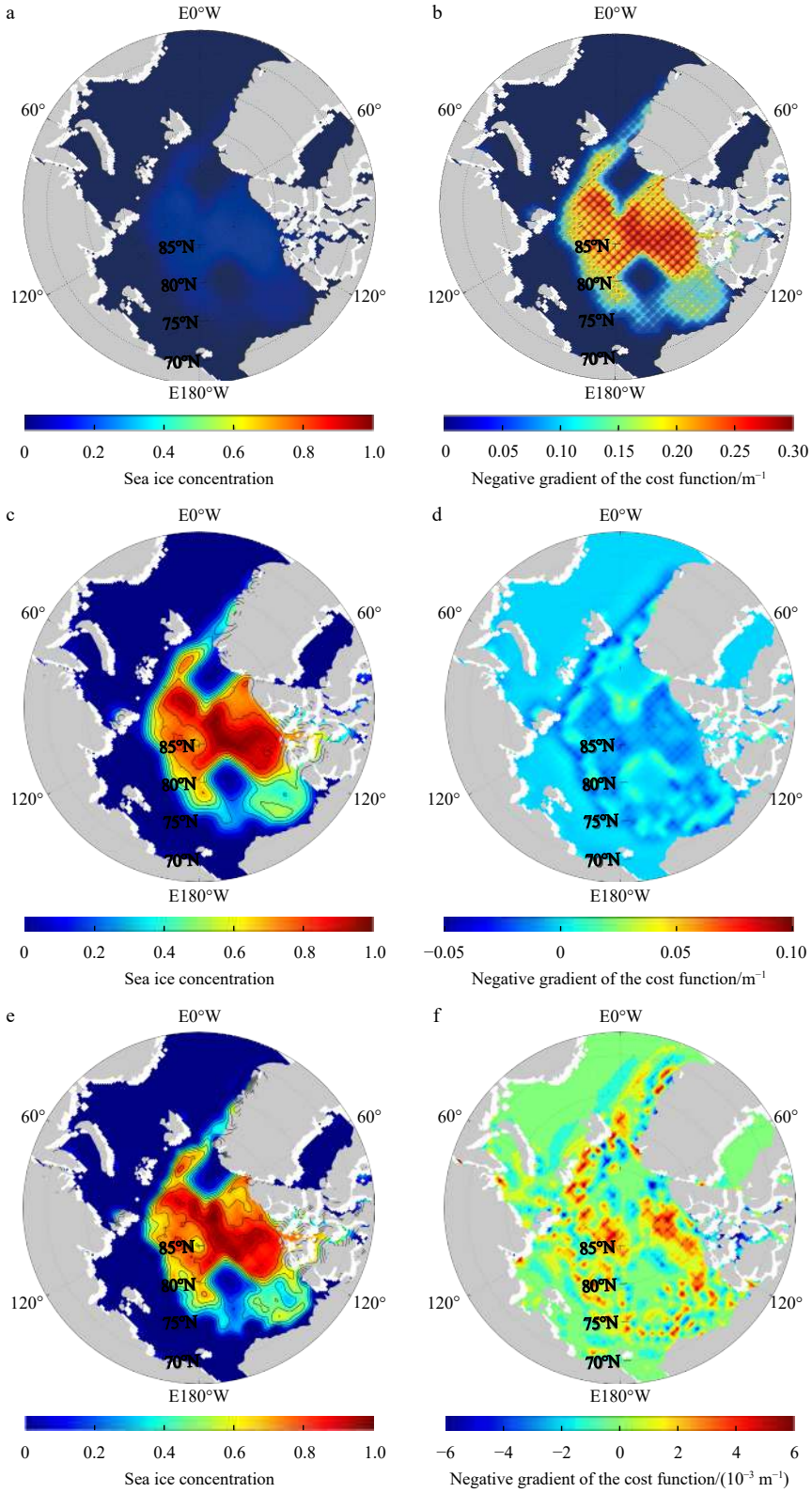

Fig. 7. Analyzed field (left column) and the descent direction ($-\nabla J$) (right column) solved using the L-BFGS scheme (β=4) at iteration 2 (a, b), 4 (c, d) and 8 (e, f), respectively.

the low-order recursive filter, which brings us several extra benefits. First, it solves the boundary problem arising from the series of the first-order recursive filter. Second, it has better filtering accuracy than low-order filters. In addition, the algorithm is easy to be parallelized since the right and left filters can be executed independently and simultaneously.

(2) As a multi-scale recursive filter 3D-VAR method, the MHRF scheme can better account for resolvable multi-scale in the observations and analyze all wavelengths once in a single iterative procedure. From the experimental results, the MHRF

scheme demonstrates its good ability to construct the analyzed field. In addition, since the right and left filters are independent, the filtering process is performed only once in each direction, which significantly increases the calculation efficiency of the assimilation process. In the future work, we try to combine the assimilation system constituted by the MHRF scheme with the sea

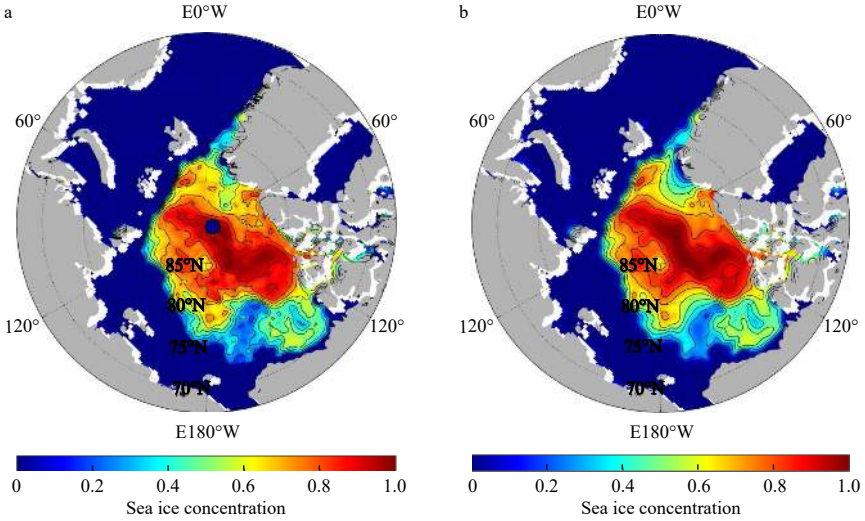

Fig. 8. The true SIC (a) and the analysis result (b) from the MHRF scheme with β =0.99 and N =125.

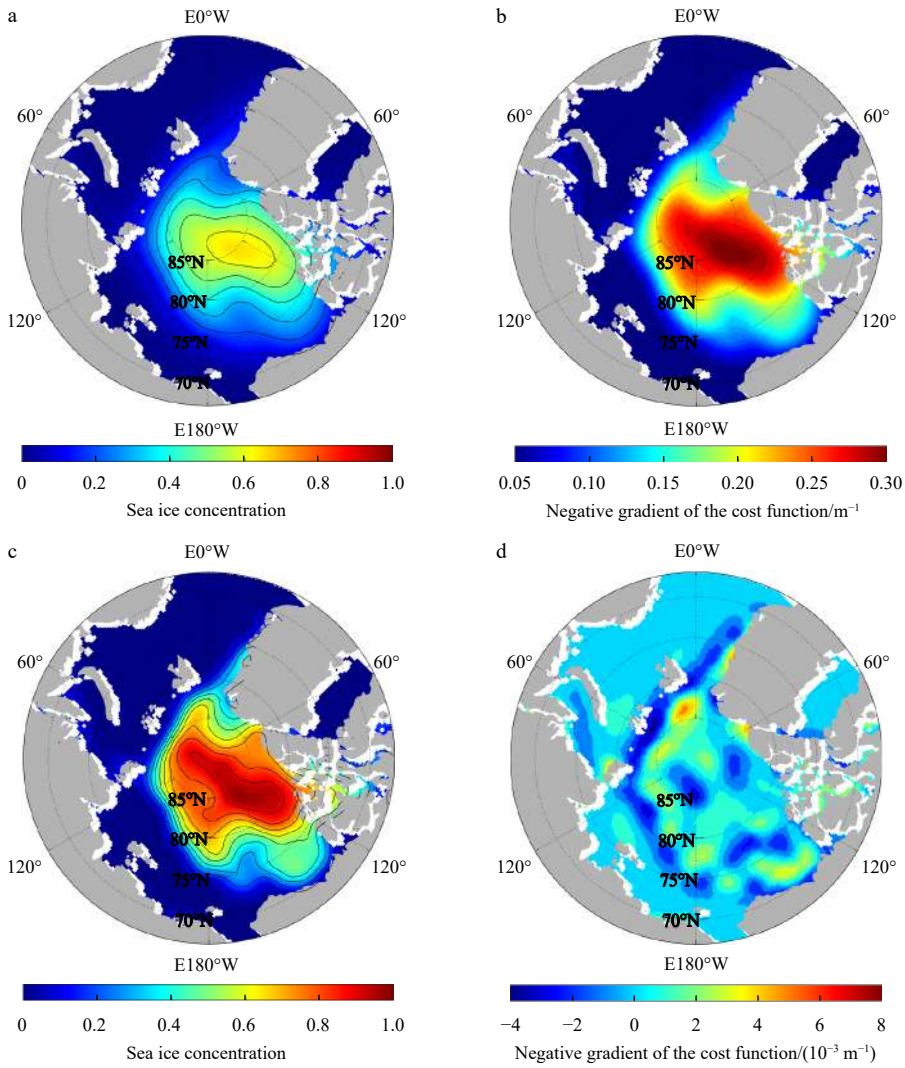

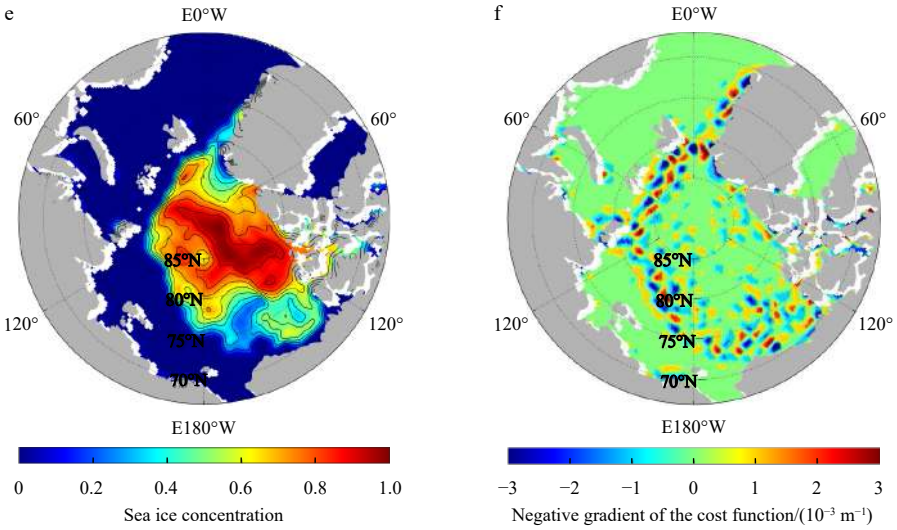

Fig. 9. Analyzed field (left column) and the descent direction (right column) of the MHRF scheme (β=0.99) at iteration 6 (a, b), 30 (c, d) and 55 (e, f).

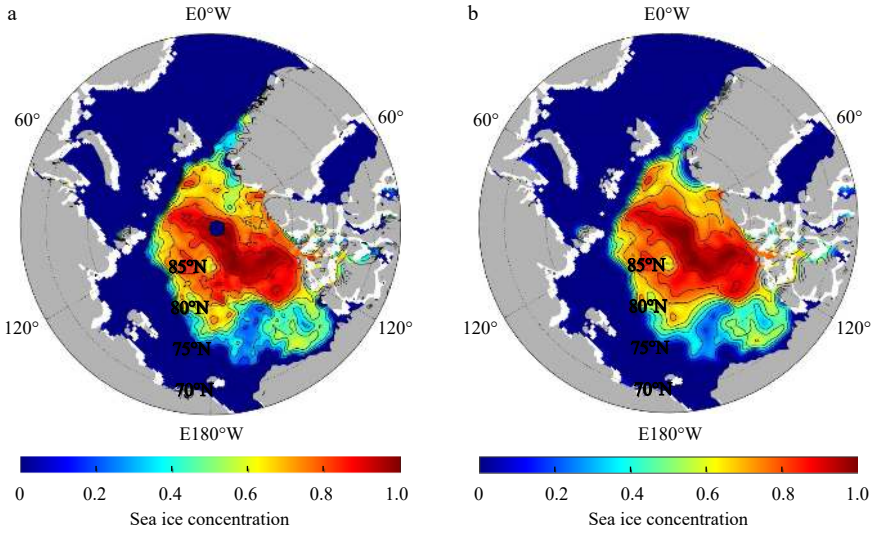

Fig. 10. The true SIC (a) and the analysis result (b) from the SMRF scheme.

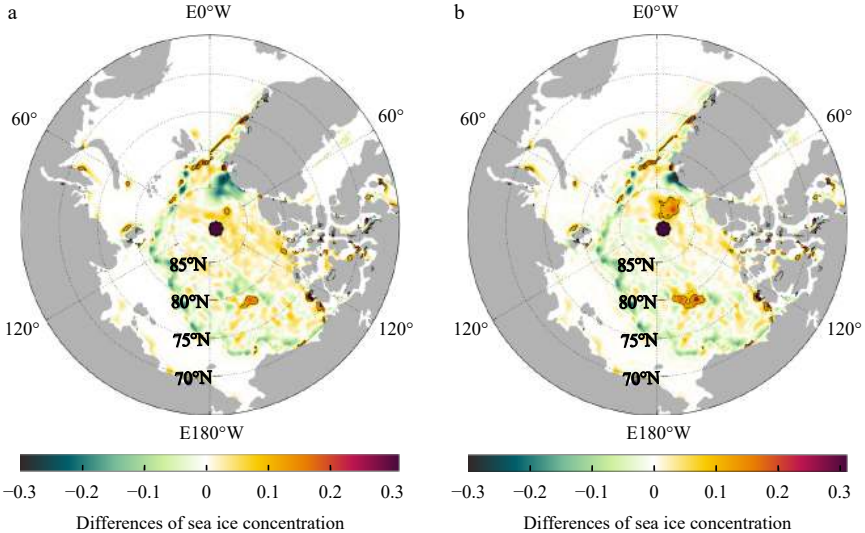

Fig. 11. The differences between the analyzed field and the true SIC field for the MHRF scheme (a) and the SMRF scheme (b).

Table 1. Comparison of RMSE and CPU computation time between the MHRF scheme and the SMRF scheme

	RMSE	The iteration steps	CPU time/s
MHRF scheme	0.059 8	125	3.303
SMRF scheme	0.058 7	500	23.438

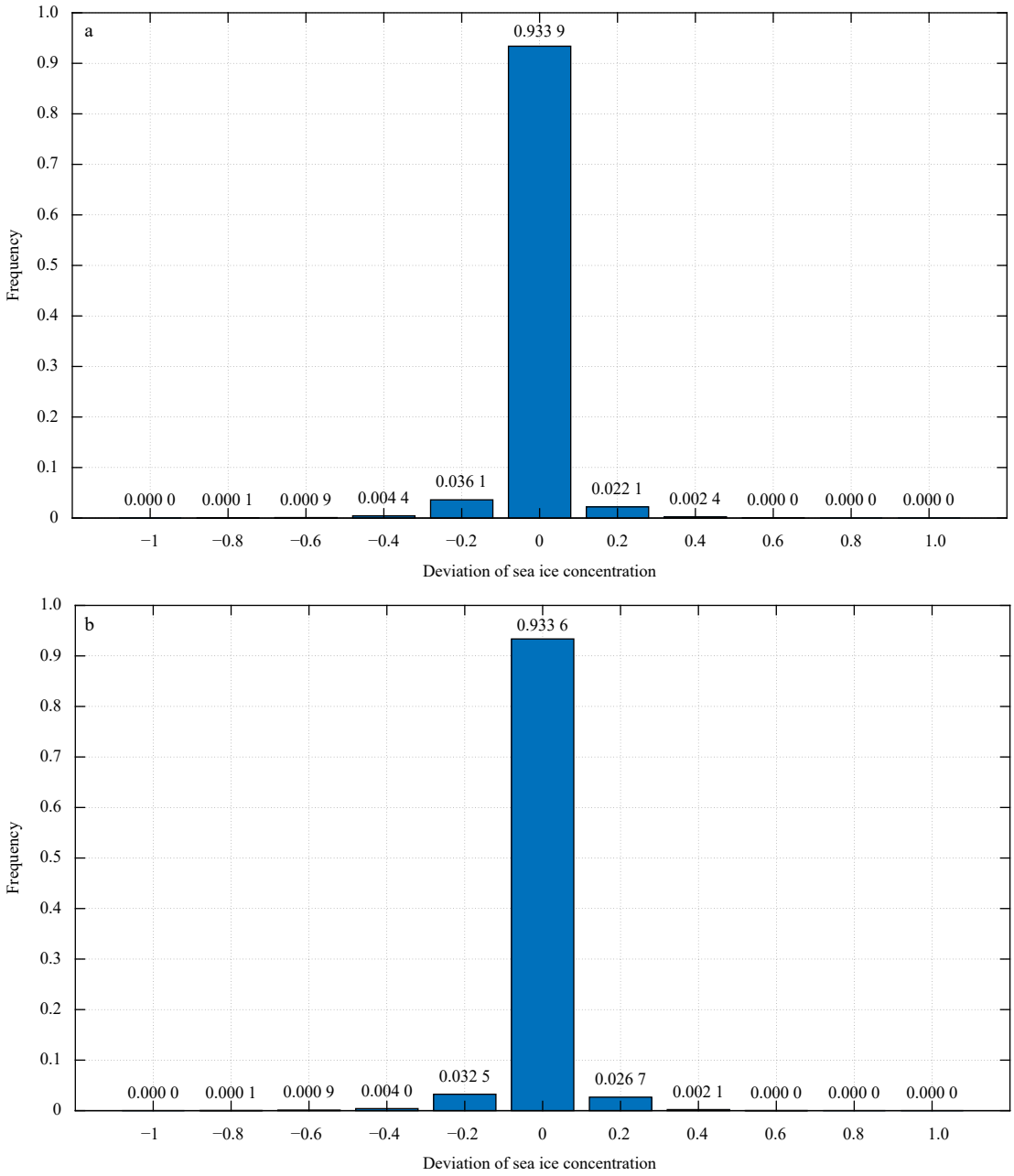

Fig. 12. Histogram of the deviation between the analyzed field and the true SIC field for the MHRF scheme (a) and SMRF scheme (b).

ice prediction system, in order to improve the prediction efficiency under the premise of ensuring the accuracy of the initial field.

(3) The filtering processes discussed in this study are based on the horizontal uniform grid, that is, for the filter with definite order, its characteristic scale is fixed and only depends on the grid scale. In the range of several hundred kilometers, the autocovariance function can indeed be assumed to be spatially homogeneous and isotropic in the horizontal direction (Zeng, 2006). However, for the more general non-uniform grid, the feature scale should change with the terrain, just like the multigrid method, which is a further goal of the MHRF scheme.

References

Cavalieri D J, Parkinson C L, DiGirolamo N, et al. 2012. Intersensor calibration between F13 SSMI and F17 SSMIS for global sea ice data records. IEEE Geoscience and Remote Sensing Letters, 9(2): 233–236, doi: 10.1109/LGRS.2011.2166754

Derber J, Rosati A. 1989. A global oceanic data assimilation system. Journal of Physical Oceanography, 19(9): 1333–1347, doi: 10.1175/1520-0485(1989)019<1333:AGODAS>2.0.CO;2

Gao Jidong, Xue Ming, Brewster K, et al. 2004. A three-dimensional variational data analysis method with recursive filter for Dop-

pler radars. Journal of Atmospheric and Oceanic Technology, 21(3): 457–469, doi: 10.1175/1520-0426(2004)021<0457:ATVDAM>2.0.CO;2

Hayden C M, Purser R J. 1995. Recursive filter objective analysis of meteorological fields: Applications to NESDIS operational processing. Journal of Applied Meteorology and Climatology, 34(1): 3–15, doi: 10.1175/1520-0450-34.1.3

He Zhongjie, Xie Yuanfu, Li Wei, et al. 2008. Application of the sequential three-dimensional variational method to assimilating SST in a global ocean model. Journal of Atmospheric and Oceanic Technology, 25(6): 1018–1033, doi: 10.1175/2007jtecho540.1

Huang Xiangyu. 2000. Variational analysis using spatial filters. Monthly Weather Review, 128(7): 2588–2600, doi: 10.1175/1520-0493(2000)128<2588:vausf>2.0.co;2

Huang Bohua, Kinter J L, Schopf P S. 2002. Ocean data assimilation using intermittent analyses and continuous model error correction. Advances in Atmospheric Sciences, 19(6): 965–992, doi: 10.1007/s00376-002-0059-z

Li Dong, Wang Xidong, Zhang Xuefeng, et al. 2011. Multi-scale 3D-VAR based on diffusion filter. Marine Science Bulletin, 30(2): 164–171, doi: 10.3969/j.issn.1001-6392.2011.02.007

Li Wei, Xie Yuanfu, He Zhongjie, et al. 2008. Application of the multigrid data assimilation scheme to the China Seas' temperature forecast. Journal of Atmospheric and Oceanic Technology, 25(11): 2106–2116, doi: 10.1175/2008JTECHO510.1

Lorenc A. 1992. Iterative analysis using covariance functions and filters. Quarterly Journal of the Royal Meteorological Society, 118(505): 569–591, doi: 10.1002/qj.49711850509

Masina S, Pinardi N, Navarra A. 2001. A global ocean temperature and altimeter data assimilation system for studies of climate variability. Climate Dynamics, 17(9): 687–700, doi: 10.1007/s003820000142

Maslanik J, Stroeve J C. 1999. Near-real-time DMSP SSMIS daily polar gridded sea ice concentrations. Boulder, CO, USA: National Snow and Ice Data Center

Moré J J, Thuente D J. 1994. Line search algorithms with guaranteed sufficient decrease. ACM Transactions on Mathematical Software, 20(3): 286–307, doi: 10.1145/192115.192132

Purser R J, McQuigg R. 1982. A successive correction analysis scheme using recursive numerical filters. Bracknell, Berkshire, UK: National Meteorological Library

Purser R J, Wu Wanshu, Parrish D F, et al. 2003a. Numerical aspects of the application of recursive filters to variational statistical analysis. Part I: Spatially homogeneous and isotropic Gaussian covariances. Monthly Weather Review, 131(8): 1524–1535, doi: 10.1175//1520-0493(2003)131<1524:NAOTAO>2.0.CO;2

Purser R J, Wu Wanshu, Parrish D F, et al. 2003b. Numerical aspects of the application of recursive filters to variational statistical analysis. Part II: Spatially inhomogeneous and anisotropic general covariances. Monthly Weather Review, 131(8): 1536–1548, doi: 10.1175//2543.1

Van Vliet L J, Young I T, Verbeek P W. 1998. Recursive Gaussian derivative filters. In: Proceedings of the Fourteenth International Conference on Pattern Recognition. Brisbane, QLD, Australia: IEEE, 509–514

Zeng Zhongyi. 2006. Inverse problems in atmospheric science. Taiwan: National Editorial Library, 306–307

Zhang Xuefeng, Yang Lu, Fu Hongli, et al. 2020. A variational successive corrections approach for the sea ice concentration analysis. Acta Oceanologica Sinica, 39(9): 140–154, doi: 10.1007/s13131-020-1654-5